

See discussions, stats, and author profiles for this publication at: <https://www.researchgate.net/publication/13358263>

# Thermal and pH-Induced Conformational Changes of a $\beta$ -Sheet Protein Monitored by Infrared Spectroscopy †

ARTICLE · BIOCHEMISTRY · MARCH 1999  
Impact Factor: 3.02 · DOI: 10.1021/bi981567 · Source: PubMed

CITATIONS  
60

READS  
49

## 6 AUTHORS, INCLUDING:

 Rosana Chehin  
National University of Tucuman  
37 PUBLICATIONS 367 CITATIONS  
[SEE PROFILE](#)

 Valery L Shnyrov  
Universidad de Salamanca  
180 PUBLICATIONS 1,727 CITATIONS  
[SEE PROFILE](#)

---

## **Thermal and pH-Induced Conformational Changes of a $\beta$ -Sheet Protein Monitored by Infrared Spectroscopy**

---

**Rosana Chehín, Ibón Iloro, María José Marcos, Enrique Villar,  
Valery L. Shnyrov, and José Luis R. Arrondo**

Grupo de Biomembranas Departamento de Bioquímica, Universidad  
del País Vasco, P.O. Box 644, E-48080 Bilbao, Spain, and  
Departamento de Bioquímica y Biología Molecular, Universidad de  
Salamanca, Plaza Doctores de la Reina s/n, 37007 Salamanca, Spain

# **Biochemistry<sup>®</sup>**

Reprinted from  
Volume 38, Number 5, Pages 1525–1530

# Thermal and pH-Induced Conformational Changes of a $\beta$ -Sheet Protein Monitored by Infrared Spectroscopy<sup>†</sup>

Rosana Chehín,<sup>‡,§</sup> Ibón Iloro,<sup>‡</sup> María José Marcos,<sup>||</sup> Enrique Villar,<sup>||</sup> Valery L. Shnyrov,<sup>||,⊥</sup> and José Luis R. Arondo\*,<sup>‡</sup>

Grupo de Biomembranas Departamento de Bioquímica, Universidad del País Vasco, P.O. Box 644, E-48080 Bilbao, Spain, and Departamento de Bioquímica y Biología Molecular, Universidad de Salamanca, Plaza Doctores de la Reina s/n, 37007 Salamanca, Spain

Received July 1, 1998; Revised Manuscript Received October 19, 1998

**ABSTRACT:** The stability of a lentil lectin, an all- $\beta$  protein, has been perturbed by changes in pH and temperature. In the pH interval 5.0 → 10.0, the overall secondary structure does not undergo significant changes. However, if the individual components of the infrared amide I band are considered, changes in band components attributed to variations in  $\beta$ -sheet and  $\beta$ -turns cross-interactions are detected. The combined effects of pH and temperature reveal that the protein is more compact at pH 7.5 with lower denaturation temperatures at pH 5.0 or 10.0, indicating a less stable protein under those conditions. According to our results, the structural stability of the  $\beta$ -sheet would depend not only on the intermolecular interactions among the strands but also on the conformation of the segments connecting these strands. The protein infrared band assignment has also been examined since the three-dimensional structure of the lentil lectin protein is known from X-ray diffraction studies. Two of the bands observed are attributed to  $\beta$ -sheet. The one at  $1620\text{ cm}^{-1}$ , not affected if the medium is deuterated, is assigned to hairpins composed by two strands connected by a rigid turn whereas that located at  $1633\text{ cm}^{-1}$  corresponds to strands associated by more flexible segments. The band appearing at  $1645\text{ cm}^{-1}$  in  $\text{H}_2\text{O}$  corresponds to the open, flexible loops that are connecting the  $\beta$ -strands. The simplest assumption of the various secondary structure components having identical IR extinction coefficients is enough to provide IR-derived data that are in good agreement with the structure solved by X-ray diffraction.

Lectins are proteins that bind carbohydrates with a high degree of specificity (1). The lectin from lentils (*Lens culinaris*) consists of two proteins LcH-A and LcH-B. These isolectins have the same molecular weight, are immunochemically identical, and display analogous hemagglutinating properties (2). Lentil lectin is bivalent with two heavy subunits ( $\beta$ -chains of about 17 kDa) and two light subunits ( $\alpha$ -chains of about 7 kDa) (3). This lectin exhibits two identical carbohydrate-binding sites that are inhibited by D-mannose, D-glucose, and their derivatives (4).

Analysis of the currently available three-dimensional structures of legume lectins suggests that all these proteins are built according to a similar model. Their main structural feature consists of two antiparallel  $\beta$ -sheets that are connected either by turns giving rise to  $\beta$ -hairpins or by longer more

flexible loops. The active protein consists of a dimer with each monomer containing one  $\alpha$ - and one  $\beta$ -chain together with a calcium and a manganese atom in the vicinity of the putative carbohydrate recognition site. The presence of these two metal ions is essential for their sugar-binding activity, and the geometry of the metal-binding sites is a very conserved feature in the different legume lectins (5).

The biological functions of proteins depend on the correct folding of their native structures, but for a protein to remain viable, it is also necessary that it possesses an overall stability. The folded conformations can be disrupted by environmental changes not involving variations in covalent structure (6). Changes in pH vary the net charge of the protein, and at extremes values, the protein unfolds by exposition of buried groups, i.e., His. At intermediate pH values, the changes in side-chain ionization produce variations in hydrogen bonding and salt bridges that could destabilize the protein although not enough as to unfold it completely. Temperature is also a destabilizing agent involving probably variations in hydrogen bonding and the van der Waals forces.

In the present work, we have used infrared spectroscopy to study the combination of pH and temperature in destabilizing a protein composed mainly of  $\beta$ -sheet, without any regular  $\alpha$ -helix and with the strands connected by turns and long loops. Infrared spectroscopy has been used to study conformational changes by looking at variations in the amide

\* To whom correspondence should be addressed. Phone: +34-946 012 485. Fax: +34-944 648 500. E-mail: gbproarj@lg.ehu.es.  
† Universidad del País Vasco.  
§ Permanent address: INSIBIO, Universidad Nacional de Tucumán, Chacabuco 461, 4000 S. M. de Tucumán, Tucumán, Argentina.

|| Universidad del Salamanca.  
|| Permanent address: Institute of Theoretical and Experimental Biophysics of Russian Academy of Sciences, 142292 Puschino, Russia.

I band arising mainly from C=O stretching vibrations from the peptidic bond (7). Moreover, because of the knowledge of the lectin crystal structure, the results are not only interpreted in terms of structural changes but they have been also used to confirm the assignment of some infrared amide I band components.

## MATERIALS AND METHODS

**Materials.** DEAE-cellulose, sodium dodecyl sulfate, dithiothreitol, horse red blood cells, methyl-D-glucoside, Hepes, succinate, and glycine buffers and D<sub>2</sub>O were purchased from Sigma (St. Louis, MO). Reagents for electrophoresis were from Bio-Rad laboratories (Richmond, CA), Sephadex G-100 was from Pharmacia (Uppsala, Sweden). All reagents were of the highest purity available. Double-distilled water was used throughout.

**Protein Purification.** Lentil seeds (*Lens culinaris*), from La Armuña area, Salamanca, Spain, were used. Lentil lectin purification was accomplished by DEAE-cellulose chromatography (8) and specific adsorption on Sephadex G-100 (2). Lentils (1 kg) obtained from local stores were soaked overnight at 4 °C in 4 L of 0.9% NaCl. The mixture was homogenized using a polytron and then centrifuged at 10800g for 20 min at 4 °C. The resulting supernatant was precipitated with ammonium sulfate between 30 and 80%. The precipitate was dissolved in 10 mM potassium phosphate buffer at pH 7.4 and dialyzed against the same buffer for 72 h with changes of medium every 8 h. The dialyzed solution was passed through a DEAE-cellulose column 5 × 40 cm with a capacity of 500 mL. The lectin was not retained by the resin. The solution obtained was then rendered 1 mM CaCl<sub>2</sub> and 1 mM MnCl<sub>2</sub> in the same buffer and chromatographed through a Sephadex G-100 column. The lectin was retained by the column and was later eluted from the gel with a 0.1 M methyl-D-glucose solution in buffer. The fractions containing the lentil lectin were pooled and dialyzed against the above-mentioned buffer and concentrated with an AMICON concentrator, through a PM-10 membrane. The purity of the sample was checked by SDS-PAGE.

**Protein Analysis.** Protein concentration determinations were performed by the Lowry procedure (9) and by ultraviolet absorption at 280 nm (8). SDS-PAGE was performed in a flat block with a polyacrylamide gradient of 5 to 25% by the method of Fairbanks et al. (10). Electrophoresis was run for 90 min at 90 V (constant). Gels were prefixed and stained using the method of Merrill et al. (11). Hemagglutinating activity was measured by a standard dilution titer assay (12).

**Infrared Measurements.** The protein samples were measured at 8 mg/mL in the following buffers: at pH (or pD) 5.0 in 10 mM phosphate-citrate, at pH 7.5 in 10 mM phosphate, and at pH 10.0 in 10 mM borax-NaOH. To transfer the protein to D<sub>2</sub>O buffer, the aqueous solution was evaporated in a Speed-vac (Savant) evaporator and then reconstituted in D<sub>2</sub>O.

The spectra were recorded in a Nicolet Magna II 550 spectrometer equipped with a MCT detector using a de-mountable liquid cell (Harrick Scientific, Ossining, NY) with calcium fluoride windows and 6 μm spacers for samples in

H<sub>2</sub>O medium or 50 μm spacers for samples in D<sub>2</sub>O medium. A tungsten–copper thermocouple was placed directly onto the window and the cell placed into a thermostated cell mount. Typically, 1000 scans for each, background and sample, were collected and the spectra obtained with a nominal resolution of 2 cm<sup>-1</sup>. Data treatment and band decomposition of the original amide I have been described previously (7, 13–16). Briefly, for each component, four parameters are considered: band position, band height, bandwidth, and band shape. Thus, in a typical amide I band decomposition with six or seven band components, the number of parameters is 24–28. The number and position of component bands is obtained through deconvolution and derivation, initial heights are set at 90% of those in the original spectrum for the bands in the wings and for the most intense component and at 70% of the original intensity for the other bands. Initial bandwidths are estimated from the Fourier derivative. The Lorentzian component of the bands is initially set at 10%. The baseline is removed prior to starting the fitting process. The iteration procedure is carried out in two steps as described (16). The mathematical solution of the decomposition may not be unique, but if restrictions are imposed such as the maintenance of the initial band positions in an interval of ±1 cm<sup>-1</sup>, the preservation of the bandwidth within the expected limits, or the agreement with theoretical boundaries or predictions, the result becomes, in practice, unique. The fitting result is evaluated (a) visually by overlapping the reconstituted overall curve on the original spectrum and (b) by examining the residual obtained by subtracting the fitting from the original curve. The methodology has also been checked with well-characterized proteins, e.g., myoglobin or concanavalin A. Besides, in some proteins that were resolved by X-ray diffraction after obtaining the secondary structure by this method, a good agreement between both results was found (14, 17).

Thermal analysis was performed in the interval 30–80 °C in 3 degree steps. At every step, the sample was left to equilibrate and the spectra measured as described above.

## RESULTS

**pH-Induced Structural Changes of the Lectin.** Protein structure is studied by infrared spectroscopy through decomposition of the conformationally sensitive infrared spectral bands arising from the peptide bond (7). The most important band in conformational studies is the amide I band which is located between 1700 and 1600 cm<sup>-1</sup> and is due mainly (~80%) to the carbonyl stretching vibration of the peptide bond. Decomposition of the original amide I band in H<sub>2</sub>O and D<sub>2</sub>O media into its constituents improves the assignment of the component bands to specific structural features (15). The result of the decomposition of the amide I' at pH 7.0, 5.0, and 10.0 in D<sub>2</sub>O is shown in Figure 1 (spectra in H<sub>2</sub>O not shown). The values obtained from the fittings in D<sub>2</sub>O and H<sub>2</sub>O at the different pHs studied are listed in Table 1.

At pH 7.5, seven bands are seen in D<sub>2</sub>O and six in H<sub>2</sub>O. Infrared band assignment is not a straightforward process because of the sensitivity of the amide I components to changes in the environment. Yet, some of the bands can be unambiguously assigned (7). In the lentil lectin, the crystal

Table 1: Band Position ( $\text{cm}^{-1}$ ) and Percentage Area (%) Corresponding to the Components Obtained after Curve Fitting the Amide I Band of the Lentil Lectin at 37 °C and Different pHs in  $\text{H}_2\text{O}$  and  $\text{D}_2\text{O}$  Media

| pH 5.0               |                            |                      |               | pH 7.4               |               |                      |               | pH 10.0              |               |                      |               |
|----------------------|----------------------------|----------------------|---------------|----------------------|---------------|----------------------|---------------|----------------------|---------------|----------------------|---------------|
| $\text{H}_2\text{O}$ |                            | $\text{D}_2\text{O}$ |               | $\text{H}_2\text{O}$ |               | $\text{D}_2\text{O}$ |               | $\text{H}_2\text{O}$ |               | $\text{D}_2\text{O}$ |               |
| band position        | band area (%) <sup>a</sup> | band position        | band area (%) |
| 1692                 | 2                          | 1691                 | 2             | 1691                 | 2             | 1691                 | 2             | 1691                 | 2             | 1686                 | 2             |
| 1679                 | 10                         | 1676                 | 8             | 1678                 | 9             | 1679                 | 5             | 1678                 | 11            | 1678                 | 4             |
| 1663                 | 16                         | 1666                 | 6             | 1661                 | 16            | 1667                 | 8             | 1663                 | 14            | 1668                 | 9             |
|                      |                            | 1656                 | 14            |                      |               | 1658                 | 15            |                      |               | 16657                | 13            |
| 1648                 | 25                         | 1646                 | 22            | 1648                 | 26            | 1646                 | 25            | 1648                 | 28            | 1646                 | 23            |
| 1633                 | 29                         | 1633                 | 32            | 1634                 | 33            | 1633                 | 35            | 1634                 | 28            | 1633                 | 34            |
| 1620                 | 18                         | 1619                 | 17            | 1620                 | 14            | 1620                 | 12            | 16220                | 16            | 1618                 | 16            |

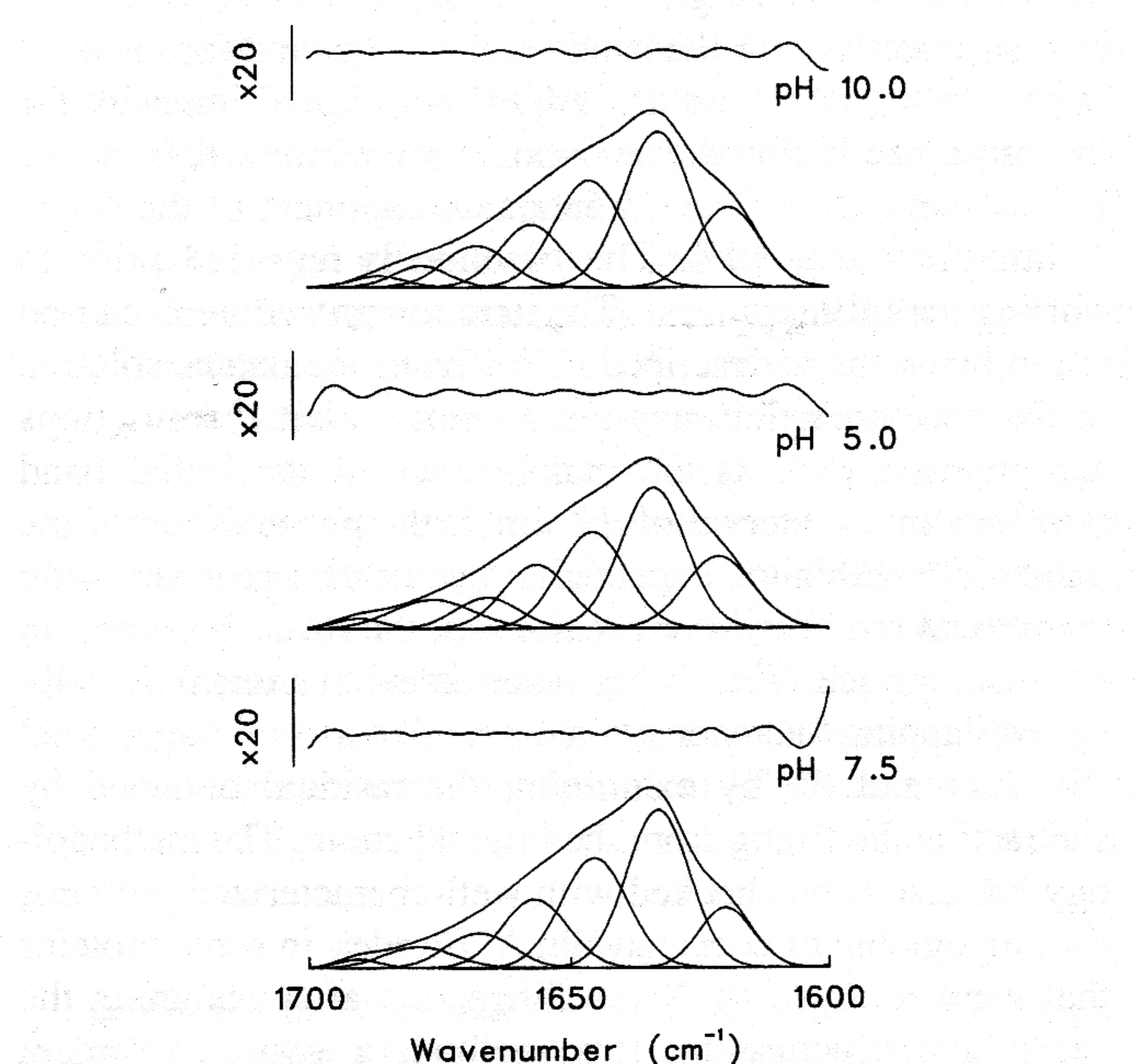


FIGURE 1: Amide I band decomposition of the lectin spectrum in  $\text{D}_2\text{O}$  buffer showing the component bands, the envelope and, in dashed lines, the reconstruction of the amide I band from the components at the different pHs studied. (A) pH 7.5; (B) pH 5.0; (C) pH 10.0. The difference between the fitted curve and the original is plotted on top of the curves expanded 20 times. Note that the dashed and continuous lines are virtually superimposed, because of the goodness of the fit, therefore they are hard to distinguish.

structure has been solved by X-ray crystallography (5), helping in the assignment of the components. Thus, the bands at 1633 and 1620  $\text{cm}^{-1}$  are characteristic of  $\beta$ -sheet structure, the major structural component of lectins. The band located at 1658  $\text{cm}^{-1}$  in  $\text{D}_2\text{O}$  is usually produced by  $\alpha$ -helix; however, bands originated from turns or even 3<sub>10</sub>-helices with dihedral angles close to  $\alpha$ -helix have also been described at this frequency (18, 19). The components located around 1668 and 1679  $\text{cm}^{-1}$  are attributed to  $\beta$ -turns. Two bands around 1620 and 1692  $\text{cm}^{-1}$  in  $\text{H}_2\text{O}$  and  $\text{D}_2\text{O}$  media, not affected by isotopic exchange, were described in a  $\beta$ -hairpin-forming peptide (20). The band around 1646  $\text{cm}^{-1}$  has been attributed to different structures. In  $\text{D}_2\text{O}$ , but not in  $\text{H}_2\text{O}$ , the unordered structure is located in this region. It has been also attributed to flexible loops (21), and this agrees better with the crystal structure according to which long loops are the connecting segments of some of the sheet strands.

Additionally, to pH 7.5, the infrared spectra of the lectin at pH 5.0 and at pH 10.0 were also measured. The values corresponding to the band fitting are also included in Table 1. The most appreciable difference is a small decrease of

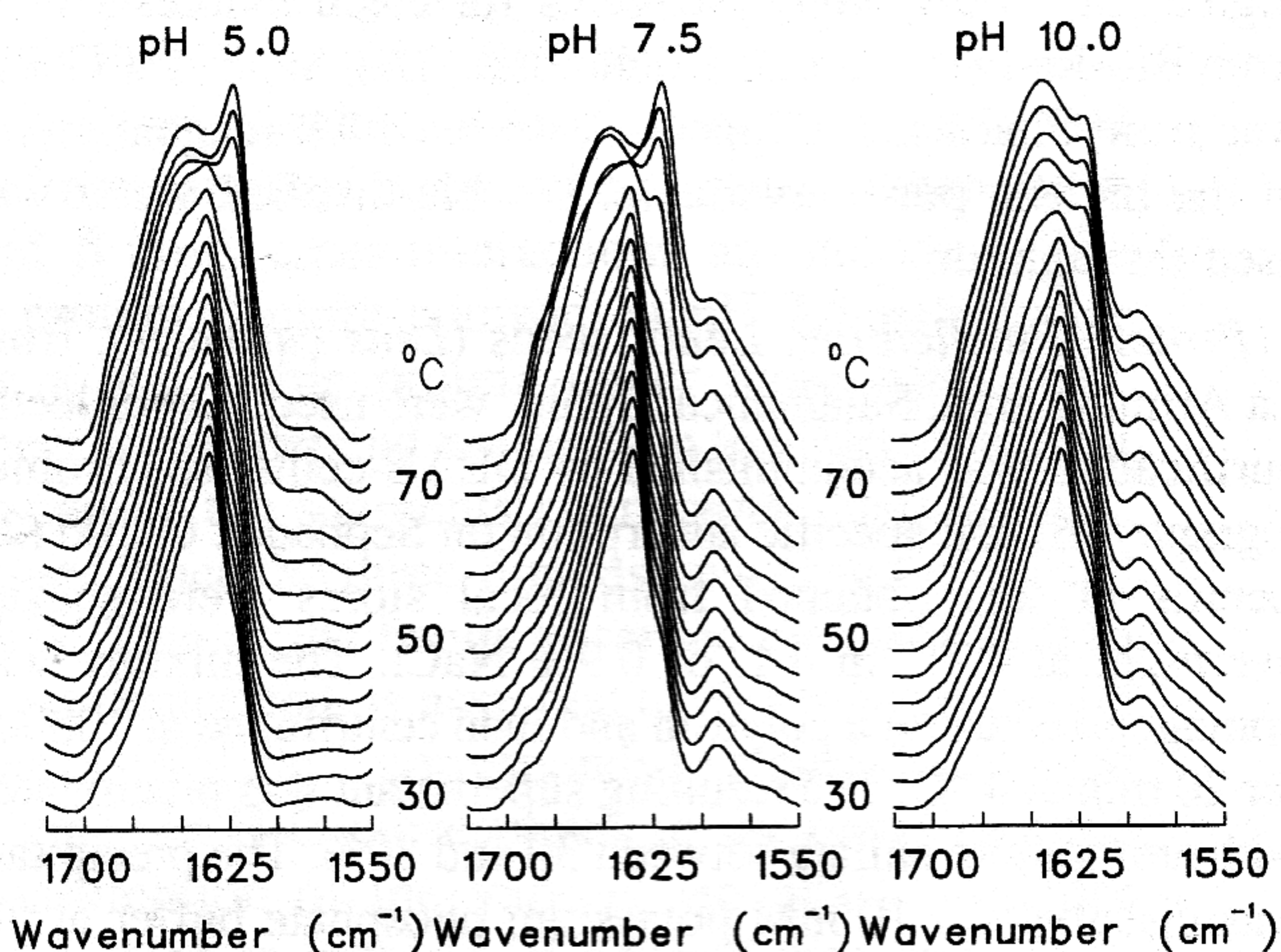


FIGURE 2: Stacked IR spectra of lentil lectin, recorded at regularly increasing temperature intervals and at various pHs. The temperature range is indicated in degrees centigrade. The spectra have been deconvolved with a halfwidth of 18 and a  $K = 2$ .

the component at 1633  $\text{cm}^{-1}$  when the pH is either increased or lowered. This difference is concomitant with changes in the band around 1620  $\text{cm}^{-1}$ . At pH 10, this band is shifted to 1618  $\text{cm}^{-1}$  in  $\text{D}_2\text{O}$  but not in  $\text{H}_2\text{O}$ , together with a shift of the high-frequency component from 1691 to 1686  $\text{cm}^{-1}$ . These observations point at pH 10.0 to a protein core more accessible to the  $\text{H} \rightarrow \text{D}$  exchange. A difference is also observed in the bands attributed to turns where shifts of 2–3  $\text{cm}^{-1}$  are produced together with small changes in band percentage. However, even if the secondary structure is roughly similar from pH 7 to 5 or 10, the protein conformation at these pHs is not alike. Thus, the bands arising from  $\beta$ -sheet structure are located around 1620, 1633, and 1690  $\text{cm}^{-1}$  and the sum of their contribution is 49% at the three pHs studied, in agreement with the crystal structure. A similar result is observed with turns, whose proportion, according to the bands around 1661 and 1678  $\text{cm}^{-1}$  in  $\text{H}_2\text{O}$  at the three pHs studied ranges 25–27%.

**Thermal Studies.** Protein thermal denaturation can be followed by infrared spectroscopy by following at the changes induced in the amide I band by temperature. Figure 2 shows the thermally induced changes produced in the lentil lectin spectra at the different pHs studied. Protein denaturation is characterized in  $\text{D}_2\text{O}$  medium by the appearance of two bands around 1620 and 1685  $\text{cm}^{-1}$ , produced by intermolecular protein–protein contacts (15). Different plots can be used to characterize the thermal profile, e.g., bandwidth vs temperature or the ratio (absorbance of the most intense component/absorbance of the emerging band) vs

Table 2: Band Position ( $\text{cm}^{-1}$ ) and Percentage Area (%) Corresponding to the Components Obtained after Curve Fitting the Amide I Band of the Lentil Lectin at 37 and 75 °C and Different pHs in  $\text{D}_2\text{O}$  Medium

| pH 5.0        |                            |               |               | pH 7.4        |               |               |               | pH 10.0       |               |               |               |
|---------------|----------------------------|---------------|---------------|---------------|---------------|---------------|---------------|---------------|---------------|---------------|---------------|
| 37 °C         |                            | 75 °C         |               | 37 °C         |               | 75 °C         |               | 30 °C         |               | 75 °C         |               |
| band position | band area (%) <sup>a</sup> | band position | band area (%) |
| 1691          | 2                          | 1684          | 4             | 1691          | 2             | 1682          | 7             | 1686          | 2             | 1682          | 6             |
| 1676          | 8                          | 1671          | 15            | 1679          | 5             | 1671          | 12            | 1678          | 4             | 1671          | 10            |
| 1666          | 6                          | 1659          | 13            | 1667          | 8             |               |               | 1668          | 9             | 1660          | 17            |
| 1656          | 14                         | 1649          | 12            | 1658          | 15            | 1659          | 16            | 16657         | 13            | 1649          | 15            |
| 1646          | 22                         | 1639          | 12            | 1646          | 25            | 1647          | 22            | 1646          | 23            | 1640          | 18            |
| 1633          | 32                         | 1632          | 25            | 1633          | 35            | 1632          | 31            | 1633          | 34            | 1630          | 15            |
| 1619          | 17                         | 1619          | 18            | 1620          | 12            | 1618          | 12            | 1618          | 16            | 1618          | 17            |

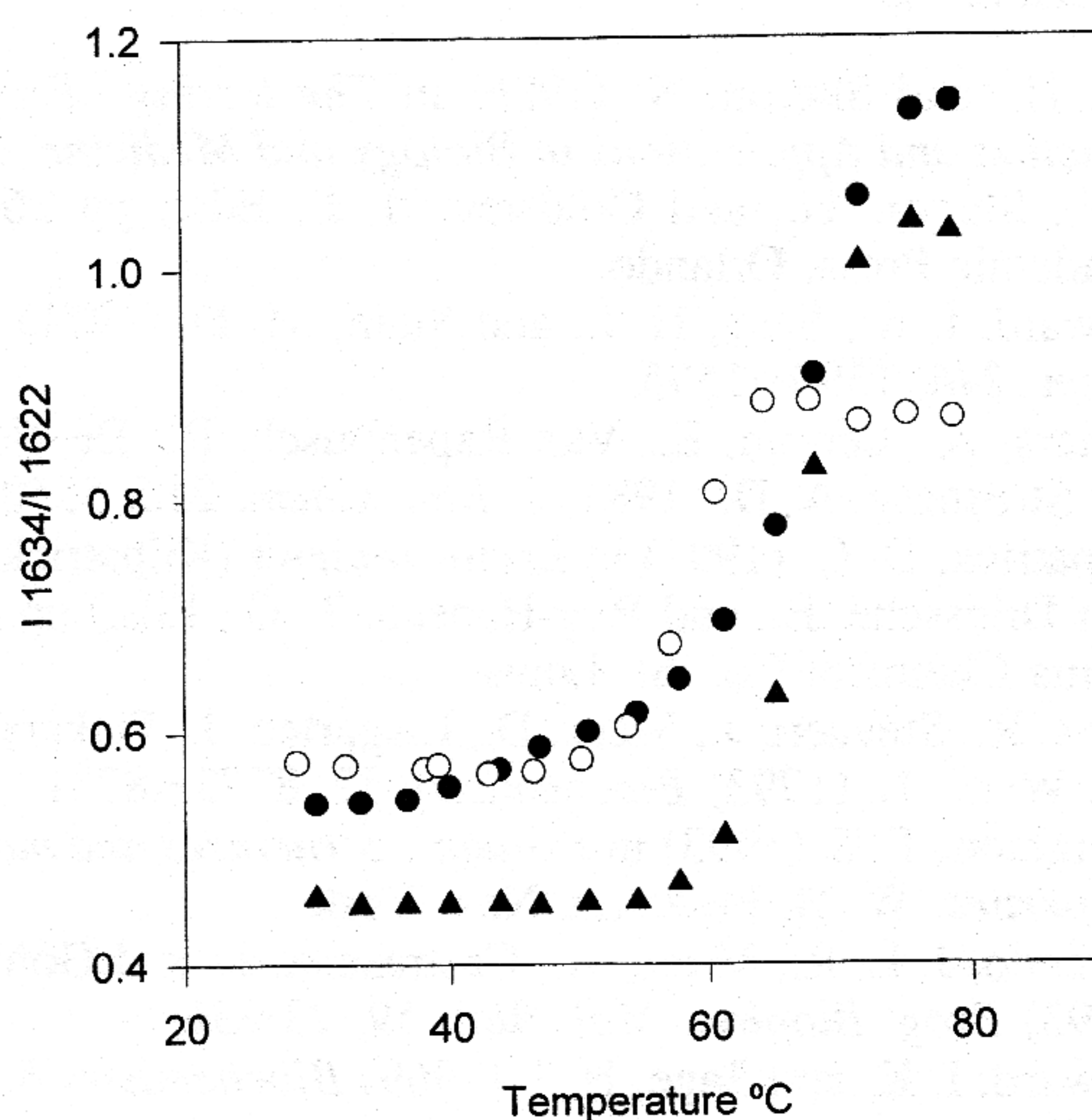


FIGURE 3: Intensity ratio vs temperature profiles of lentil lectin IR spectra corresponding to pH 7.5 (▲), pH 5.0 (●), and pH 10.0 (○).

temperature (22). The latter has been used in Figure 3 to visualize the thermal profile of the lectin denaturation at the pHs studied. The plot for the protein at pH 7.0 shows that denaturation starts around 60 °C with a midpoint around 66 °C and its shape is evocative of a cooperative process. This thermal event would correspond to the main transition observed previously by DSC at about 70 °C (23). The temperature at which irreversible denaturation is produced in proteins, either measured by DSC (23, 24) or IR spectroscopy (25), depends on the heating rate. Thus, the step heating in the infrared experiments leads to a lower heating rate as compared with DSC and the denaturation temperatures are correspondingly lower (26, 27). A small and broad transition observed by DSC around 50 °C is not observed at pH 7 by infrared spectroscopy, probably because of the intrinsic differences between both techniques: DSC will reveal only cooperative changes arising from any region in the protein, while IR data will respond to both cooperative and noncooperative phenomena but only if the amide bond protein backbone is involved. However, at pH 5.0 the profile is more complex with two thermal events, one starting at 45 °C and then the major event at 67 °C. At pH 10.0, the beginning of the thermal denaturation is at around 55 °C. Denaturation does not give rise to only one structure, the postdenaturation conformation depends instead of the denaturation history of the sample (Table 2) as observed previously in other proteins (17, 28). The lower denaturation temperature observed at pH 10 agrees with the structural characteristics described above for this pH. The results of

thermal denaturation corroborate the different protein structure of the lectin at the three pHs considered.

## DISCUSSION

**Protein Stability.** The lentil lectin is an all- $\beta$  protein with no significant proportions of  $\alpha$ -helix. It can be considered as representative of a family of proteins with high denaturation temperatures and is considered to be a highly stable entity. Variation of pH in the 5–10 range does not lead to major changes in the  $\beta$ -sheet structure of the lectin, but produces small alterations in the amide I band components that, together with the pH-induced changes of the thermal profiles, indicate changes in the protein tertiary structure. The scarcity of charged amino acids in the  $\beta$ -sheet strands (only R43, E119, and D140) would explain the small effect of pH upon this secondary structure. Most of the charged amino acids are located in the loops connecting the strands. However, the infrared spectrum does not show major differences in the amount of loops when the pH is changed, what can be accounted for the flexibility of such loops that can accommodate the electrostatic variations by changing their tertiary structure. The band located at 1620  $\text{cm}^{-1}$  and not subjected to isotopic shift has been found in a hairpin forming peptide (20). More recently, two types of  $\beta$ -turns have been elucidated by NMR in hairpins (29), and this band would correspond to the more rigid hairpins involving cross-strand side-chain interactions. These hairpin-associated turns have at least one charged amino acid residue that would be affected by the pH changes producing a different strand–strand interaction. A similar behavior with pH and temperature has been described in an  $\alpha/\beta$  protein, a  $\beta$ -glycosidase, where the increase in pH from 7 to 10 does not change the secondary structure as measured by circular dichroism, but enzyme activity is lost concomitant with a decrease in thermal stability (30).

The profile of thermal denaturation at pH 7.5 involves the aggregation of the protein at temperatures above 71 °C with a decrease in the content of loops and  $\beta$ -sheet and an increase in the bands related to aggregation and turns. At pH 5.0 below the pI, where the protein is more positively charged, the thermal profile is more complicated, but the start of denaturation is clearly at a lower temperature, indicating a less stable protein. The decrease of  $\beta$ -sheet content after denaturation at pH 5 is even greater than at pH 7.5 (Table 2) which can be associated to a less compact protein. The thermal profile of the lectin at pH 10.0 is similar to that at pH 7.5, but again denaturation starts at a lower temperature.

After denaturation, the residual  $\beta$ -sheet is decreased and aggregation is greater than at pH 7.5.

The picture that can be inferred from the infrared results on the effect of pH changes upon this  $\beta$ -sheet protein is that the protein is particularly compact (stable) at pH 7.5, with a high denaturation temperature. Increase or decrease in pH implies variation in the topology of loops and turns changing the forces stabilizing the strands and the tertiary structure of the protein. These changes do not affect the secondary structure, but the interactions between strands are weakened, thus decreasing the denaturation temperature. The destabilizing effect of pH is similar on the acidic and the basic sides, because the number of positively and negatively charged amino acids located in the turns and loops is roughly similar.

**Assignment of the Amide I Components.** One of the problems that are still not fully solved in the study of protein structure by infrared spectroscopy is band assignment. The sensitivity of band position to variations of intra- and intermolecular interactions and band coupling give rise to more component bands in the amide I than secondary structure elements. Therefore, one important point in the present study can be to relate the observed bands with the structures described in the crystal structure. The lectin structure main pattern comprises two large antiparallel  $\beta$ -sheets comprised by strands stretched out over the whole lectin dimer accounting for 45% of the protein structure and including 5 hairpins; the  $\beta$ -sheet strands are connected by loops and  $\beta$ -turns. Two low-frequency bands in the infrared spectrum at 1620 and 1633  $\text{cm}^{-1}$  are attributable to the  $\beta$ -sheet structure. The band at 1633  $\text{cm}^{-1}$  is assigned to antiparallel  $\beta$ -sheet (31), and the band at 1620  $\text{cm}^{-1}$  was first assigned in concanavalin A to  $\beta$ -edge (32) and was found later in a hairpin-forming peptide (20). The five  $\beta$ -sheet strands connected by hairpins would account for the relative proportion ( $\sim 15\%$ ) of the 1620  $\text{cm}^{-1}$  band (Table 1). The two bands for the  $\beta$ -sheet structure would imply two different populations of  $\beta$ -sheet strands. A recent  $^1\text{H}$  NMR study (29) of designed peptides has found that they can fold in aqueous solution into two different structures, one with a type I  $\beta$ -turn and the other with a type I + G1  $\beta$ -bulge turn. The result is that the turn conformation affects the cross-strand side-chain interactions. In the infrared spectrum, the appearance of the band around 1620  $\text{cm}^{-1}$  is accompanied by a lack of the isotopic shift of the high-frequency component, which would point to a more rigid connection between the strands. The  $\beta$ -strands connected by more flexible segments agree in position with the theoretical values for  $\beta$ -sheet, near 1633  $\text{cm}^{-1}$  (33), because these studies are made for noninterconnected strands of infinite length. The band around 1645  $\text{cm}^{-1}$  in  $\text{H}_2\text{O}$  is not clearly assigned and has been variously attributed to  $3_{10}$  helix (34), flexible loops (21), and more recently to helix-helix coupling in coiled coils (35). This band is close in  $\text{D}_2\text{O}$  to the value of the unordered structure and can be confused with it in studies made only in  $\text{D}_2\text{O}$  medium. From the three-dimensional picture, the structures contributing to this band are the large loops connecting some of the  $\beta$ -strands. The amount of structure involved in this region of the infrared spectrum is matched by the proportion of amino acid residues in these loops, and this band is clearly affected by protein denaturation, even under mild conditions, as could be expected from a flexible structure.

Another subject of controversy in the interpretation of infrared spectra is whether the extinction coefficients of the different structural components of the amide I have similar values (7, 36) or not (37). In the work presented, we have assumed that the extinction coefficients are the same for the various bands making up the amide I envelope and the percentages obtained are in good agreement with the values for secondary structure obtained from the X-ray diffraction data. This supports the simplest hypothesis of the similarity of IR absorptivities of the various secondary structure elements and reinforces the applicability of IR spectroscopy to quantitative structural studies in proteins.

## REFERENCES

- Lis, H., and Sharon, N. (1986) in *The lectins: Properties, Function and Applications in Biology and Medicine*. (Liener, I. E., Sharon, N., and Goldstein, I. J., Eds.) pp 266–370, Academic Press, Orlando.
- Howard, I. K., Sage, H. I., and Stein, M. D. (1971) *J. Biol. Chem.* 246, 1590–1595.
- Foriers, A., Lebrun, E., Van Rapenbusch, R., De Neve, R., and Strosberg, A. D. (1981) *J. Biol. Chem.* 256, 5550–5560.
- Kilpatrick, D. C. (1991) in *Lectin reviews* (Kilpatrick, D. C., Van Driessche, E., and Bog-Hansen, T. C., Eds.) pp 69–80, Sigma Chemical Co., St. Louis.
- Loris, R., Steyaert, J., Maes, D., Lisgarten, J., Pickersgill, R., and Wyns, L. (1993) *Biochemistry* 32, 8772–8781.
- Creighton, T. E. (1993) in *Proteins. Structures and molecular properties*, W. H. Freeman, New York.
- Arrondo, J. L. R., Muga, A., Castresana, J., and Goñi, F. M. (1993) *Prog. Biophys. Mol. Biol.* 59, 23–56.
- Howard, I. K. and Sage, H. I. (1969) *Biochemistry* 8, 2436–2441.
- Lowry, O. H., Rosebrough, N., Farr, A. L., and Randall, R. J. (1951) *J. Biol. Chem.* 193, 265–275.
- Fairbanks, G., Steck, T. L., and Wallach, D. F. H. (1971) *Biochemistry* 10, 2606–2617.
- Merril, C. R., Goldman, D., Sedman, S. A., and Ebert, M. H. (1981) *Science* 211, 1437–1438.
- Barret, T. and Inglis, S. C. (1985) in *Virology: A practical approach* (Mahy, B. W. J., Ed.) pp 119–150, IRL Press, Oxford, Washington, DC.
- Castresana, J., Muga, A., and Arrondo, J. L. R. (1988) *Biochem. Biophys. Res. Commun.* 152, 69–75.
- Arrondo, J. L. R., Muga, A., Castresana, J., Bernabeu, C., and Goñi, F. M. (1989) *FEBS Lett.* 252, 118–120.
- Arrondo, J. L. R., Castresana, J., Valpuesta, J. M., and Goñi, F. M. (1994) *Biochemistry* 33, 11650–11655.
- Bañuelos, S., Arrondo, J. L. R., Goñi, F. M., and Pifat, G. (1995) *J. Biol. Chem.* 270, 9192–9196.
- Echabe, I., Haltia, T., Freire, E., Goñi, F. M., and Arrondo, J. L. R. (1995) *Biochemistry* 34, 13565–13569.
- Bandekar, J. (1992) *Biochim. Biophys. Acta* 1120, 123–143.
- Krimm, S. and Bandekar, J. (1986) *Adv. Protein Chem.* 38, 181–364.
- Arrondo, J. L. R., Blanco, F. J., Serrano, L., and Goñi, F. M. (1996) *FEBS Lett.* 384, 35–37.
- Fabian, H., Naumann, D., Misselwitz, R., Ristau, O., Gerlach, D., and Welfle, H. (1992) *Biochemistry* 31, 6532–6538.
- Martínez, A., Haavik, J., Flatmark, T., Arrondo, J. L. R., and Muga, A. (1996) *J. Biol. Chem.* 271, 19737–19742.
- Shnyrov, V. L., Marcos, M. J., and Villar, E. (1996) *Biochem. Mol. Biol. Int.* 39, 647–656.
- Davoodi, J., Wakarchuk, W. W., Surewicz, W. K., and Carey, P. R. (1998) *Protein Sci.* 7, 1538–1544.
- Echabe, I. and Arrondo, J. L. R. (1995) in *Spectroscopy of Biological Molecules* (Merlin, J. C., Turrell, S., and Huvenne, J. P., Eds.) pp 123–126, Kluwer Academic Publishers, Dordrecht.
- Haltia, T., Semo, N., Arrondo, J. L. R., Goñi, F. M., and Freire, E. (1994) *Biochemistry* 33, 9731–9740.

27. Fernandez-Ballester, G., Castresana, J., Arondo, J. L. R., Ferragut, J. A., and Gonzalez-Ros, J. M. (1992) *Biochem. J.* 288, 421–426.
28. Taneva, S. G., Caaveiro, J. M. M., Muga, A., and Goñi, F. M. (1995) *FEBS Lett.* 367, 297–300.
29. De Alba, E., Rico, M., and Jiménez, M. A. (1997) *Protein Sci.* 6, 2548–2560.
30. D'Auria, S., Rossi, M., Nucci, R., Irace, G., and Bismuto, E. (1997) *Proteins* 27, 71–79.
31. Susi, H., and Byler, D. M. (1986) *Methods Enzymol.* 130, 290–311.
32. Arondo, J. L. R., Young, N. M., and Mantsch, H. H. (1988) *Biochim. Biophys. Acta* 952, 261–268.
33. Susi, H. (1969) in *Structure and Stability of Biological Macromolecules* (Timasheff, S. N., and Stevens, L., Eds.) pp 575–663, Dekker, New York.
34. Miick, S. M., Martinez, G. V., Fiori, W. R., Todd, A. P., and Millhauser, G. L. (1992) *Nature* 359, 653–655.
35. Reisdorf, W. C., Jr., and Krimm, S. (1996) *Biochemistry* 35, 1383–1386.
36. Byler, D. M., and Susi, H. (1986) *Biopolymers* 25, 469–487.
37. De Jongh, H. H. J., Goormaghtigh, E., and Ruysschaert, J. M. (1996) *Anal. Biochem.* 242, 95–103.

BI981567J